Conductivity and Structure of a Polyamide/Silver Iodide Nanocomposite

Yoshie Fujimori,[1] Yasuo Gotoh,[1] Akio Kawaguchi,[2] Yutaka Ohkoshi,[1] Masanobu Nagura[1]

[1]*Faculty of Textile Science and Technology, Shinshu University 3-15-1 Tokida, Ueda, Nagano 386-8567, Japan*
[2]*Research Reactor Institute, Kyoto University, Kumatori, Osaka 590-0494, Japan*

Received 16 June 2007; accepted 15 October 2007
DOI 10.1002/app.27601
Published online 25 February 2008 in Wiley InterScience (www.interscience.wiley.com).

ABSTRACT: In this study, the structure and properties of an organic–inorganic composite material prepared from nylon 6 doped with fine particles of silver iodide (AgI) were examined. The preparation of the composite involved the complexation of nylon 6 with polyiodide ions such as I_3^- and I_5^- by immersion in an iodine/potassium iodide (I_2–KI) aqueous solution followed by reaction in a silver nitrate ($AgNO_3$) aqueous solution; this resulted in the *in situ* formation of β-AgI fine particles within the nylon 6 matrix. The AgI content formed in the composite was dependent on the immersion temperatures of the I_2–KI and $AgNO_3$ solutions. Lower solution temperatures resulted in larger amounts of AgI in the composite. This method readily provided a composite with a high content of AgI in nylon 6 and a conductivity of approximately 10^{-5} Ω^{-1} cm^{-1}. In a uniaxially oriented nylon 6 matrix, AgI particles precipitated with anisotropic shape, which was caused by the orientation of the precursor polyiodide ions. The structure of the oriented composite provided the anisotropic conductivity. Additionally, the composite exhibited high antibacterial properties. The procedure used in this study is considered a unique method for the preparation of organic–inorganic composites. © 2008 Wiley Periodicals, Inc. J Appl Polym Sci 108: 2814–2824, 2008

Key words: inorganic materials; nanocomposites; nylon

INTRODUCTION

The synthesis and properties of silver iodide (AgI) have been actively researched, mainly due to its properties of photosensitivity and superionic conductivity.[1–3] Generally, AgI crystals exhibit three phases, designated as α, β, and γ, under atmospheric pressure and in order of decreasing temperature.[4] At room temperature and ambient atmospheric pressure, the two phases β-AgI and γ-AgI may exist. In β-AgI, which is stable below 147°C, the iodine ions are arranged in a hexagonal close-packed lattice with the silver ions being tetrahedrally coordinated to each of the iodides (a wurtzite structure). In γ-AgI, the iodine ions are arranged in a face-centered cubic lattice with the silver ions tetrahedrally coordinated to the iodine ions, and γ-AgI transforms to β-AgI at 137°C. Above 147°C, β-AgI transforms into α-AgI, in which the iodine ions form a body-centered cubic lattice. The level of ionic conductivity of α-AgI is extremely high and comparable to those of liquid electrolytes ($\approx 10^0$ Ω^{-1} cm^{-1}). Since the discovery of this high conductivity,[5] AgI has been called a *solid superionic conductor* and has attracted wide interest. In contrast, β-AgI and γ-AgI, which are stable at lower temperatures, exhibit ionic conductivities that are six orders of magnitude lower than that of α-AgI. Attempts have been made to obtain AgI or its composites with higher ionic conductivities at room temperature. For example, the pseudobinary system of AgI (90.1 mol %)–Ag_3BO_3 (9.9 mol %) has superionic α-AgI stabilized at room temperature by a melt-quenching technique and exhibits high ionic conductivity of about 10^{-1} Ω^{-1} cm^{-1}.[6] The compounding of rubidium iodide with AgI ($RbAg_4I_5$) resulted in a conductivity on the order of 10^{-1} Ω^{-1} cm^{-1}.[7,8] A new type of AgI with a structure similar to that of a mixture of β-AgI and γ-AgI was also reported to show a high conductivity of 10^{-3} Ω^{-1} cm^{-1}.[9] The conductivity of AgI depends not only on the crystal form but also on the particle size. That is, smaller particles of silver halides exhibit higher ionic conductivities, and therefore, much attention has recently been paid to the preparation and characterization of AgI nanoparticles.[10–14]

Nowadays, high-function and high-performance materials are demanded in various fields such as energy-saving, resource-saving optics and electrical and electronic engineering. Organic/inorganic hybrids or nanocomposite materials have been actively developed to obtain new properties that each

Correspondence to: Y. Gotoh (ygotohy@shinshu-u.ac.jp).
Contract grant sponsor: Japan Science Society (through a Sasakawa Scientific Research Grant).
Contract grant sponsor: Ministry of Education, Culture, Sports, Science, and Technology (through a Grant-in-Aid for the Global Center of Excellence (COE) Program).

component does not show independently. Representative of such materials are nanocomposite materials composed of inorganic nanoparticles introduced into an organic polymer matrix. These nanocomposites, with introduced nanosized metal and semiconducting particles, have very different properties, such as characteristic optical, electrical, and magnetic properties caused by the quantum size effect,[15–19] from those of the bulk composite materials. We reported preparative methods and optical properties for some nanocomposites with nanoparticles (e.g., silver metal, silver sulfide, copper sulfide, copper iodide) introduced into a matrix of nylon 6 or poly(acrylic acid).[20–22]

AgI is an attractive inorganic compound, and thus, AgI is considered a good candidate for a component of nanocomposite materials. Composites with AgI introduced into an inorganic matrix have been reported; for example, AgI nanoparticles were precipitated *in situ* in nanopores of alumina prepared by the anodizing process.[23] As a result, the crystal transition from β-AgI to α-AgI interestingly occurred at a higher temperature (160°C) compared with that of bulk AgI (147°C) because the nanopores of the alumina matrix strongly restricted the thermal motion of AgI. However, few researchers have reported nanocomposites of AgI in organic polymer matrices, although it is expected that the properties of AgI particles in a nanocomposite would be different from the bulk properties.

We successfully prepared a nylon 6/AgI composite via a precursor complex of polymer–polyiodide ions and briefly reported some interesting properties.[24] For example, the transition temperature of β-AgI to α-AgI for the composite was more than 20°C lower than that of bulk AgI (147°C). The ionic conductivity of the composite was much higher than that of pure β-AgI or γ-AgI, although the volume fraction of AgI in the insulating nylon 6 matrix was only about 20%. AgI was formed in the nylon 6 matrix by the reaction of precursor polyiodide ions I_n^- (n = 3, 5,...) with Ag^+ ions and the subsequent *in situ* precipitation of AgI.

However, accumulated results from the study of nylon 6/AgI composites have not yet been reported in detail. This article deals with the influence of the preparation conditions for AgI formation in a nylon 6 matrix via a nylon 6/polyiodide ion complex on the properties of the resulting composites. That is, we examined conditions, such as the immersion temperature of the iodine/potassium iodide (I_2–KI) or silver nitrate ($AgNO_3$) aqueous solutions and the molecular orientation of nylon 6 chains, that influenced the amount, structure, and properties of AgI formed in nylon 6, and we also investigated the reaction mechanism of polyiodide ions and Ag^+ ions.

EXPERIMENTAL

Materials

Biaxially stretched nylon 6 (random nylon 6) film (Unitika Co., Ltd., Japan) with a thickness of 15 μm showed a random distribution of the crystallite orientation in the film plane. Uniaxially stretched nylon 6 (drawn nylon 6) film was prepared with nylon 6 pellets (Toray Industries, Inc.) by compression with a hot-press machine at 255°C and 5 MPa followed by the quenching of the film in ice water. The quenched film was then drawn in an oven at 150°C and annealed for 2 h. The resulting film thickness was about 40 μm.

Iodine (I_2), potassium iodide (KI), and $AgNO_3$ were purchased from Wako Pure Chemical Industries, Ltd.

Sample preparation

The preparation of nylon 6/AgI composites was performed with the following method. First, a nylon 6 film was immersed in I_2–KI aqueous solution (I_2 = 0.15 mol/L, KI = 3.3 mol/L) at a prescribed constant temperature to obtain a dark brown nylon 6/polyiodide complex film. (This process is called *primary doping*.) Second, the complex film was immersed in a 1 mol/L $AgNO_3$ aqueous solution at a prescribed constant temperature. (This process is called *secondary doping*.) Consequently, AgI fine particles were formed in the nylon 6 matrix, and a pale yellowish composite film was obtained. The prepared composites were then washed with distilled water. For the drawn nylon 6 film, the film was fixed with a Teflon plate to prevent shrinkage of the samples during each doping process. The immersion time of random nylon 6 films was 1 h for both the primary and secondary doping, whereas the immersion time for the drawn nylon 6 films was 1 h for the primary doping and 4 h for the secondary doping. These doping times were within the saturation conditions for each doping. The longer doping time for the drawn nylon 6 film was attributed to the larger film thickness.

Neat bulk AgI powder for comparison was prepared by the mixture of $AgNO_3$ and KI aqueous solutions with equivalence. The molar ratio of Ag and I of the neat AgI was 1.00, which was determined by energy dispersive X-ray analysis, which indicated the high purity of AgI.

Measurements

X-ray diffraction (XRD) profiles were obtained with a Rigaku Rotaflex RU-200B X-ray generator equipped with a Rigaku PMG-GA goniometer. The X-ray source was Ni-filtered Cu Kα radiation (0.15418 nm) generated at 40 kV and 150 mA. X-ray

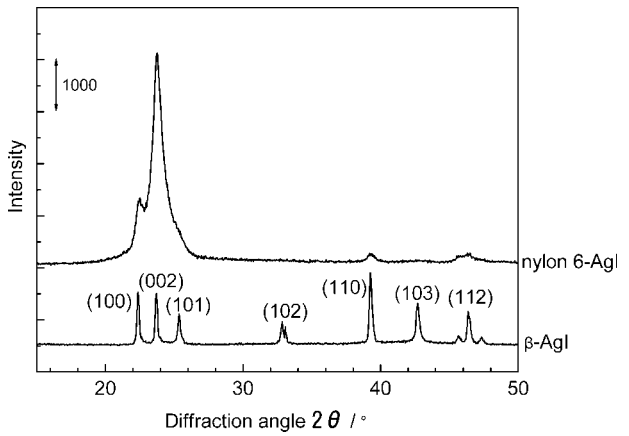

Figure 1 XRD patterns of nylon 6/AgI and β-AgI powder.

photographs were taken using a Rigaku R-AXIS-DS3 imaging plate system.

Small-angle X-ray scattering (SAXS) images were obtained with the synchrotron radiation X-ray of beam line of a BL-15A instrument in the Photon Factory of the High Energy Accelerator Research Organization. The applied X-ray wavelength was 0.15 nm. The diameter of the X-ray beam was 0.35 mm (vertical) × 0.53 mm (horizontal) at the focus point. The SAXS image was taken by a 1000 × 1018 pixel charge coupling device camera. The camera length was determined with lead stearate. The intensity profiles along the diffraction angle (2θ) were taken from the obtained SAXS image.

Electrical conductivity was obtained by an alternating current process with an electrical resistance measurement system (ITK Co., Japan, DVA-225). The frequency was 1 krad/s (ca. 159 Hz). The electrode spacing was 1 cm, and the sample size was 3 cm long and 1 cm wide. Platinum was sputtered as an electrode on the sample because of diminishing contact resistance. The measurement was conducted by a two-point method after the checking of standard resistors. Impedance measurement was carried out with a Solartoron 1296 and an SI 1260 system.

Scanning electron microscopy (SEM) observation was conducted on a Hitachi S-2380N. The sample cross section was prepared with a microtome with a diamond knife.

Polarized Raman spectroscopy was measured with an S. T. Japan, Inc., HoloLab-5000 instrument equipped with an MK-II filtered probe head with an Nd : YAG laser beam of 532 nm generated at 50 mW. The measurement was carried out under a resolution of 2.5 cm^{-1}, an exposure time of 3 s, and a summation of 10 times.

Thermogravimetric (TG) analysis was measured with a Rigaku ThermoPlus II at a heating rate of 10°C/min in an air flow.

Antibacterial properties were evaluated on the basis of the JIS L 1902 protocol. The colony forming units of bacteria on the culture media with the composite were measured after incubation at 37°C for 18 h. The composite used in this measurement was prepared by the immersion of nylon 6 in the I_2–KI solution at 20°C for 1 min and the $AgNO_3$ solution at 20°C for 5 min.

RESULTS AND DISCUSSION

Dependence of AgI formation on the treatment temperature

Figure 1 shows an XRD pattern of the nylon 6/AgI composite film and bulk β-AgI powder. The crystal form of AgI was basically assigned as β-AgI;[25] however, the presence of γ-AgI and other crystal forms could not be completely excluded because the main diffraction peaks of γ-AgI overlapped with those of β-AgI, which was difficult to distinguish. In this study, the crystal form of AgI was represented as β-AgI for convenience. From the XRD pattern of the composite, the width of the diffraction peaks was much broader, which indicated that the crystallinity of AgI was considerably lower than that of bulk AgI.

First, we studied the influence of the immersion temperature of the I_2–KI aqueous solution for primary iodine doping on the amount of AgI formed in the nylon 6/AgI film. The immersion temperature of the secondary doping $AgNO_3$ aqueous solution was fixed at 20°C for this measurement. The resulting composite films were flexible, and the strength was high enough that the materials could be handled. Figure 2 indicates the weight gain of the composites and the volume fraction of AgI in the composites prepared at different immersion temperatures of

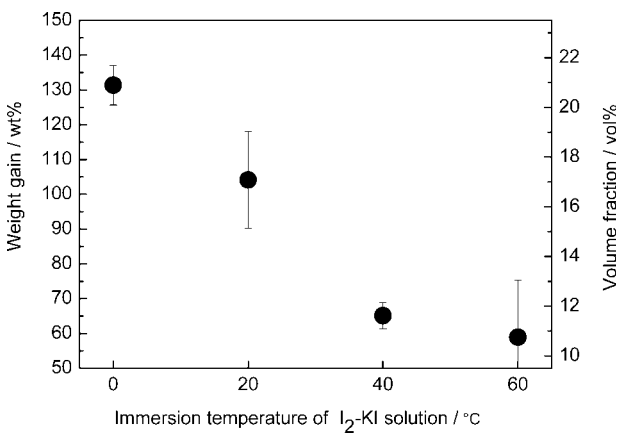

Figure 2 Dependence of the weight gain of nylon 6/AgI, or the volume fraction of AgI in nylon 6/AgI, on the immersion temperature of the I_2–KI aqueous solution (the $AgNO_3$ aqueous solution temperature was fixed at 20°C).

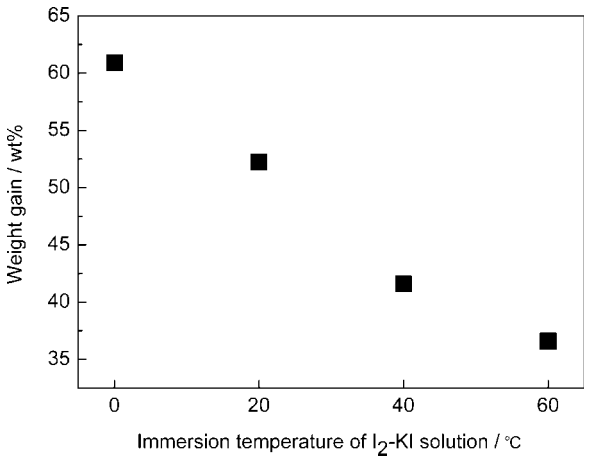

Figure 3 Dependence of the weight gain of nylon 6 doped with iodide ion on the immersion temperature of the I_2–KI aqueous solution.

I_2–KI aqueous solution. The weight gain was determined by the calculation of the difference between the weights of the nylon 6 and nylon 6/AgI films. The samples were stored at 25°C and 65% relative humidity overnight before the weight measurements. The moisture contents for each sample and the neat nylon 6 were almost 3 wt %; thus, the influence of the moisture content was small. So we calculated the weight gain without consideration of moisture content (the same holds for Figs. 3 and 4). The weight gain for each composite was measured with three or four sample sheets, and the error bar was determined from scattered values. Lower immersion temperatures of the I_2–KI aqueous solution resulted in greater weights of the nylon 6/AgI films. The weight gain of the composites prepared at immersion temperatures of 0 and 20°C were 130 and 105 wt %, respectively. These values exceed the weight of the nylon 6 matrix and were extremely high for a filler material. The content of AgI in the composite could also be arbitrarily controlled by changing the concentration of the I_2–KI solution.

To elucidate the relation of the weight gain from AgI with the immersion temperature of the I_2–KI solution, the amount of sorbed iodine component was measured because the iodine component was converted to AgI. Figure 3 shows the dependence of the amount of iodide component sorbed in the nylon 6 film on the immersion temperature for primary iodine doping. The amount of sorbed iodide component was obtained by the weight change of the nylon 6 to nylon 6/iodide complex after sufficient drying at room temperature under reduced pressure. In this case, potassium ions were contained as a counter ion of iodide ions in the nylon 6/iodide complex film, but the amount of the potassium component was very limited; for example, only 1.6 wt % of potassium ions were contained in the nylon 6/iodide complex film immersed in KI–I_2 solution at 20°C. Thus, the content of potassium is ignored in this discussion. The weight gain after primary doping due to the iodide component increased with decreasing immersion temperature. This meant that the complexation of nylon 6 with polyiodide ions such as I_3^- and I_5^- occurred more readily at lower temperature, which agreed with the fact that the iodide component was sorbed more easily at lower temperatures.[26,27] For each composite, the amount of AgI in the nylon 6/AgI composite was approximately twice that of the sorbed iodide component in the nylon 6 film. Consequently, the amount of iodide component reflected the amount of AgI in the resultant film.

Next, the influence of the immersion temperature of the $AgNO_3$ aqueous solution for secondary silver doping on the amount of AgI formed in nylon 6 film was studied. Figure 4 shows the weight gain of composites prepared at different immersion temperatures of the $AgNO_3$ solution. In this case, the immersion temperature of the I_2–KI solution was fixed at 20°C. Weight gain was achieved by the same procedure as that used for the results presented in Figure 2. The weight gain of nylon 6/AgI increased with decreasing temperature for secondary doping, as shown in Figure 4. However, the rate of change in the amount of AgI formed in the composites was less dependent on the immersion temperature of the $AgNO_3$ solution, compared with the temperature dependence of primary iodine doping. Therefore, the amount of AgI in the composite film depended more on the amount of doped iodine component. A lesser amount of AgI resulted from a higher secondary doping temperature, and it was confirmed that a small amount of AgI was dissolved in the $AgNO_3$ aqueous solution. The cross section of a nylon 6/AgI

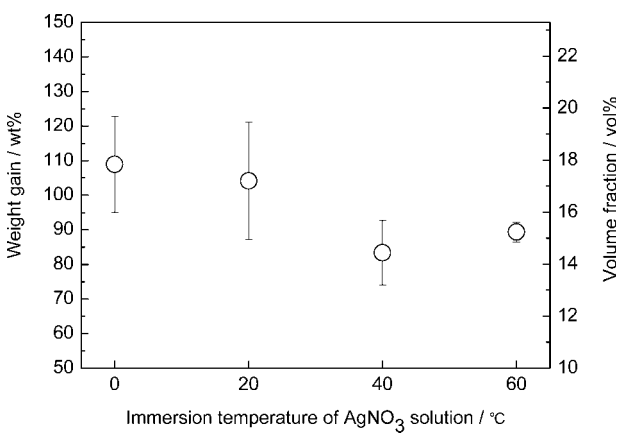

Figure 4 Dependence of the weight gain in nylon 6/AgI, or volume fraction of AgI in nylon 6/AgI, on the immersion temperature of the $AgNO_3$ aqueous solution (the I_2–KI aqueous solution temperature was fixed at 20°C).

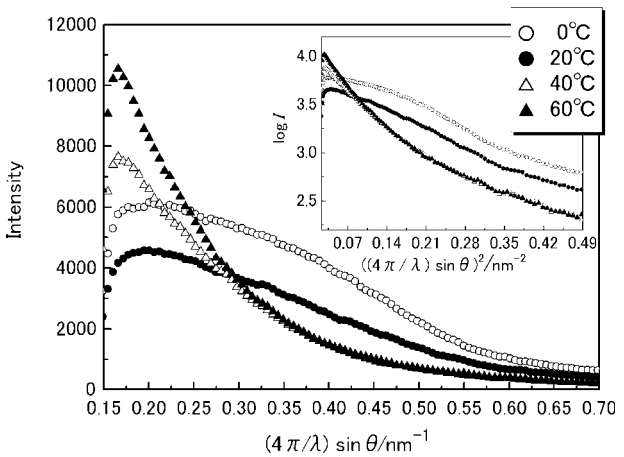

Figure 5 SAXS profiles of nylon 6/AgI films prepared from $AgNO_3$ aqueous solutions at different temperatures (the I_2–KI aqueous solution temperature was fixed at 20°C).

composite was observed by SEM, and AgI particles were not observed near the film surface. In addition, the weight gain of the nylon 6/AgI composite decreased for immersion times longer than 1 h in the $AgNO_3$ solution.

The state of the AgI particles present in the composite films was investigated next. Although the weight of AgI in nylon 6 was increased, the transparency of the nylon 6/AgI composite increased with decreasing secondary doping immersion temperature; transmittances at 600 nm for the composites prepared at secondary doping temperatures of 0 and 60°C were 73 and 29%, respectively (primary doping temperature = 20°C). These results imply that the size of AgI in the composite was smaller when the composite was immersed at a lower secondary doping temperature. Figure 5 shows SAXS profiles of nylon 6/AgI prepared at different $AgNO_3$ solution immersion temperatures. These profiles were plotted as scattering intensity (I) versus [$(4\pi/\lambda) \times \sin\theta$], and the inset figure shows Guinier plots {log I versus [$(4\pi/\lambda) \times \sin\theta]^2$}. The Guinier plots exhibited a nonstraight line for the scattering profiles, which indicated an inhomogeneous size distribution of AgI particles in nylon 6/AgI. The smallest radius of inertia of the particles in the composites was estimated from the slope of the straight line drawn between 0.15 and 0.25 nm^{-2} in [$(4\pi/\lambda) \times \sin\theta]^2$ and was about 5 nm. Thus, the size of the smallest AgI particle was estimated as about 10 nm. The SAXS profiles of the composites prepared at secondary doping temperatures of 40 and 60°C showed an increase in intensity at lower angles, below 0.10 nm^{-2} in [$(4\pi/\lambda) \times \sin\theta]^2$, which implied that there were larger AgI particles. From these observations, we considered that the decrease in the transparency of nylon 6/AgI was caused by the coarsening of the AgI particles, which led to the scattering of visible light.

This method is a simple way to impart conductivity to insulating nylon 6 by doping with AgI. Thus, we investigated the influence of the immersion temperature of the doping solution on the conductivity of the composites. Figure 6(a,b) shows the dependence of the conductivity of the nylon 6/AgI composites on the immersion temperature in $AgNO_3$ and I_2–KI aqueous solutions. The samples in this figure are the same as those presented in Figures 2 and 4. For comparison, the conductivity of a bulk β-AgI tablet prepared by compression molding was also measured. The conductivity of the bulk β-AgI was 4.1×10^{-7} Ω^{-1} cm^{-1} and was approximately in agreement with a previously reported value (3×10^{-7} Ω^{-1} cm^{-1}).[10,28] The conductivities of the composites increased with decreasing immersion temperature and were in the range 3.8×10^{-6} to 5.8×10^{-5} Ω^{-1} cm^{-1}. Interestingly, these values were more

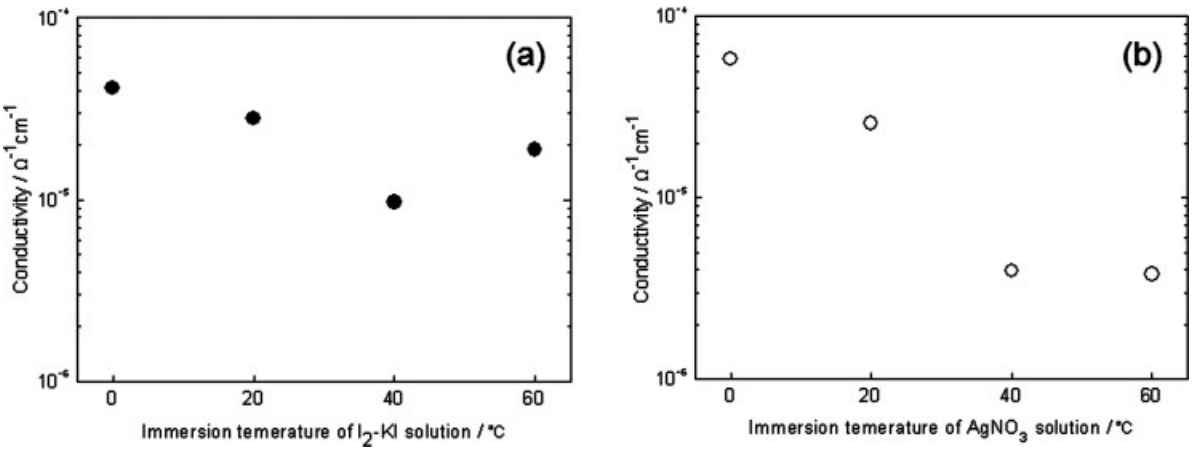

Figure 6 Dependence of the conductivity of nylon 6/AgI on the immersion temperature of (a) I_2-KI and (b) $AgNO_3$ aqueous solutions.

than one order higher than that of bulk β-AgI. When Figures 6(a) and 2 are compared, it seems that the conductivity was proportional to the amount of AgI introduced when only the temperature of the I_2–KI solution was changed; the conductivity doubled as the amount of AgI present in the composite was doubled. On the other hand, when Figures 6(b) and 4 are compared, the change of the immersion temperature of the $AgNO_3$ solution caused a larger rate of change in conductivity, although the rate of weight change of AgI was smaller than that in the case of the immersion temperature dependence of the I_2–KI solution.

Generally, the effective conductivity for a two-component mixture depends on the mixing mode, and the crudest limits have the following formulas;[10,29]

$$\sigma_L^{-1} = (1 - \nu_2)\sigma_1^{-1} + \nu_2\sigma_2^{-1} \quad (1)$$

$$\sigma_U = (1 - \nu_2)\sigma_1 + \nu_2\sigma_2 \quad (2)$$

where L and U of subscripts are respectively, the abbreviations of the lower and upper bounds, and ν_i and σ_i are the volume fraction and the conductivity of the i-th component, respectively. Equation (2) is frequently applied to interpret the total conductivity of a composite system.[30,31] The volume fraction of the AgI component contained in the composite was calculated with the density of β-AgI (5.71 g cm^{-3}),[32] and it ranged from 13 to 20 vol %. The total conductivities of the nylon 6/AgI composites were calculated with eq. (1) or eq. (2), and the conductivities of bulk β-AgI (4.1×10^{-7} Ω^{-1} cm^{-1}) and nylon 6 (1×10^{-15} Ω^{-1} cm^{-1})[33] and the densities of bulk β-AgI and nylon 6 (1.14 g/cm^3).[33] Consequently, the conductivities ranged from 1.1×10^{-15} to 1.3×10^{-15} Ω^{-1} cm^{-1} for eq. (1) and from 4.3×10^{-8} Ω^{-1} cm^{-1} to 8.5×10^{-8} Ω^{-1} cm^{-1} for eq. (2). The measured conductivity of the composite was at least two orders larger than the calculated value. This showed that the conductivity of β-AgI in the nylon 6/AgI composite was significantly higher than that of bulk β-AgI. The value of σ_U in eq. (2) was obtained from a parallel model (i.e., conductive components in the composite system were in contact throughout the sample and formed a conductive path). Thus, the conductivity of AgI particles in the composite was measured with an impedance analyzer. As a result, the conductivity was approximately 10^{-1} Ω^{-1} cm^{-1}. The high conductivity of the AgI particles was near that of α-AgI rather than that of β-AgI. This value may have been related to the AgI particle size. It has been reported that the ionic conductivity of halides of silver or copper is strongly dependent on the particle size.[10,34] A smaller particle size provides a larger ionic conductivity. For example, when the size of AgBr particles was changed from 1 to 0.3 μm, the conductivity increased from about 7×10^{-7} Ω^{-1} cm^{-1} to about 20×10^{-7} Ω^{-1} cm^{-1}.[34] In the case of AgI, the conductivity at room temperature increased decreasing particle size, that is, 1.4×10^{-4} Ω^{-1} cm^{-1} for 140 nm, 6.7×10^{-5} Ω^{-1} cm^{-1} for 160 nm, 4.0×10^{-5} Ω^{-1} cm^{-1} for 440 nm, and 7.0×10^{-6} Ω^{-1} cm^{-1} for 680 nm.[10] As shown in Figure 5, the size of the AgI particles was larger than at least 20 nm; therefore, there is a possibility that the small size of the AgI particles was related to the high ionic conductivity.

The structure of the AgI crystal is considered to be another significant factor of the high conductivity. The ion transport mechanism of AgI is attributed to lattice defects, so it was anticipated that a more disordered crystal lattice would impart a higher ionic conductivity. As shown in Figure 1, the crystallinity of AgI was considerably low; in other words, the AgI of the composite contained many lattice defects. When the nylon 6/AgI was annealed at 160°C, the diffraction peaks of β-AgI became sharper, the crystallinity increased, and the conductivity was reduced by one order of magnitude. We, therefore, considered that the high defect density was likely one factor of the high ionic conductivity of AgI in the composite. Also, a highly conductive structure of AgI at room temperature has been reported.[35,36] AgI usually possesses substructures of a sequence of hexagonal close-packed β-AgI (2H) and of a sequence of cubic close packed γ-AgI (3C). Davis et al. reported a polytype structure of 21H[37] and 7H,[38] and Lee at al. reported a 7H structure.[35] They described that the 7H polytype structure of AgI was responsible for the significant enhancement of conductivity in a composite of AgI embedded in a Al_2O_3 matrix [ca. 10^{-3} Ω^{-1} cm^{-1}, AgI : Al_2O_3 (40 m/o)].[35] The 7H structure can be approximately considered as a heterostructure alternation of β-AgI and γ-AgI (i.e., β/γ/β/γ/β/γ, ...). If space charge effects at a given β/γ interface in such a heterostructure can be assumed, most silver ions would then be disordered and effective as charge carriers, which would explain the significant conductivity enhancement in the composite.[36] These polytype structures exhibited some diffraction peaks, but it was difficult to recognize them in our composite because they were obscured by other diffraction peaks (β-AgI or nylon 6) or were of very weak intensity. However, the possibility of an AgI polytype structure in our composite could not be excluded. At any rate, we considered that the high conductivity was related to both the particle size and the crystallite structure.

Formation of anisotropic AgI in an oriented nylon 6 film

We investigated the influence of the orientation of the nylon 6 matrix on the formation of AgI. AgI particles

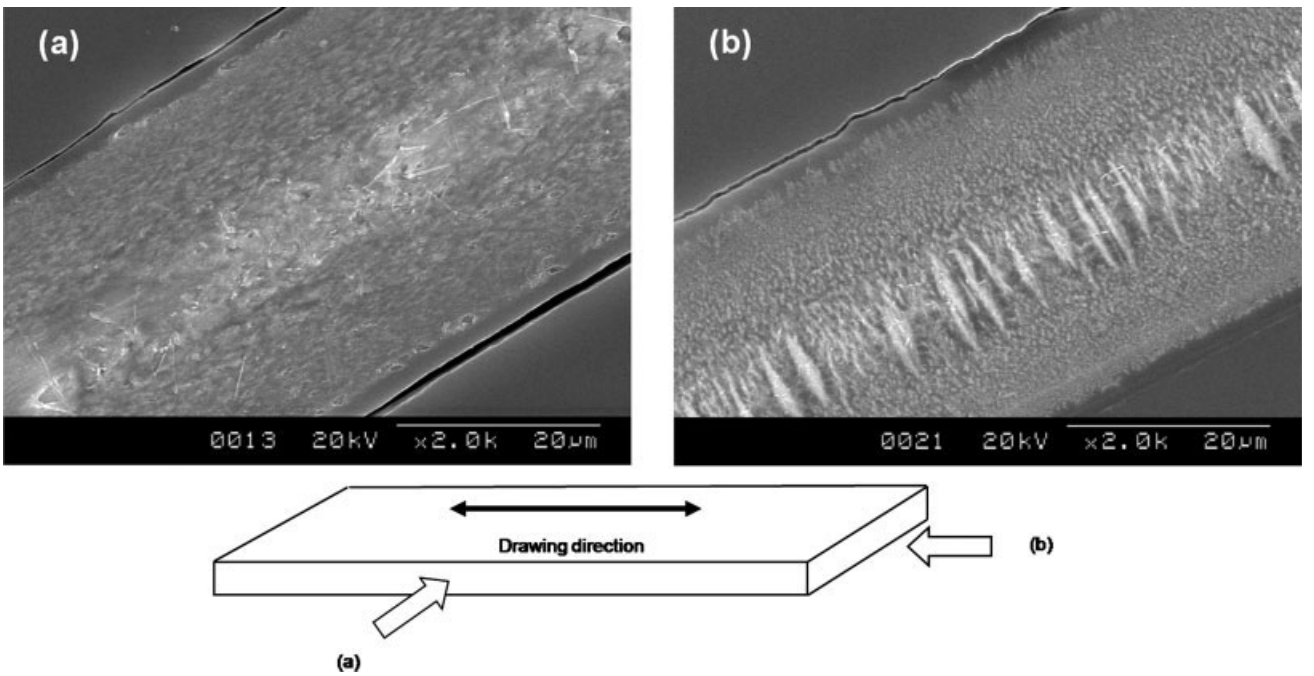

Figure 7 Cross-sectional SEM images of drawn nylon 6/AgI: (a) parallel and (b) perpendicular to the direction of drawing.

in the drawn composite film were observed by SEM. Figure 7(a,b) shows the cross-sectional SEM images of the drawn composite film with cross sections parallel and perpendicular to the direction of drawing. In the figures, the white grains are AgI particles, which were densely distributed in the composite except at the film surface. Larger anisotropic AgI grains were in the central part of the film, and smaller anisotropic AgI gains were situated around the larger AgI grains. The size of the AgI particles gradually decreased in closer proximity to the film surface. The inhomogeneous size distribution of AgI particles may have been related to the distribution of polyiodide ions because the migration speed of polyiodide ions into nylon 6 was abnormally fast,[39] and a large amount of iodine component was entered due to the strong interaction between nylon 6 and iodine.

Figure 8(a–d) shows the XRD photographs of a random nylon 6 film, a random nylon 6/AgI composite film, a drawn nylon 6 film, and a drawn nylon 6/AgI composite film, respectively. The incident X-ray beam was focused from the direction normal to the film surface. In Figure 8(b), the diffraction assigned to β-AgI is shown as Debye–Scherrer rings, which indicates that the crystallite orientation of AgI was random in the film plane. On the other hand, for the drawn composite film shown in Figure 8(d), the diffractions from β-AgI exhibited a preferred crystallite orientation. This crystallite orientation of AgI was dependent on the orientation of the nylon 6 molecule. Precursor polyiodide ions were sorbed with orientation influenced by the orientation of the nylon 6 molecular chains.[40,41] Figure 9 shows the polarized Raman spectra of the drawn nylon 6 film after primary iodine doping. The angles between the polarized plane of the laser and the drawn direction of the nylon 6 were 0 (parallel), 30, 60, and 90° (perpendicular). A strong band assigned to I_5^- (170 cm^{-1}) was observed at 0°, whereas the band at 230 cm^{-1} (assigned to I_3^-) was mainly observed with perpendicular polarization. This means that polyiodide ions were oriented as shown in Figure 9, and this agreed well with reports by Murthy and coworkers[42,43] and Lee and Porter.[44] Linear I_5^- ion chains existed in the complex with the long axes parallel to the chain axis. Linear I_3^- ion chains existed with the long axes perpendicular to the chain axis. We considered that the orientation of polyiodide ions caused the crystallite orientation and anisotropic particles of AgI. This consideration was supported by the following result. We attempted to introduce AgI into a silk fibroin fiber, which is a natural polyamide with a high crystallite orientation. However, the silk fibroin fiber could only sorb polyiodide ions in the amorphous part with low molecular orientation, and AgI particles with random orientation were formed by the reaction with Ag^+ ions during secondary doping.[45] Therefore, we considered that the orientation of AgI in the drawn composite was influenced by orientation of the polyiodide ions.

Because the anisotropy of AgI in a nylon 6 matrix may provide anisotropically conductive properties, the electrical conductivity of the drawn composite was measured. Figure 10 shows the temperature

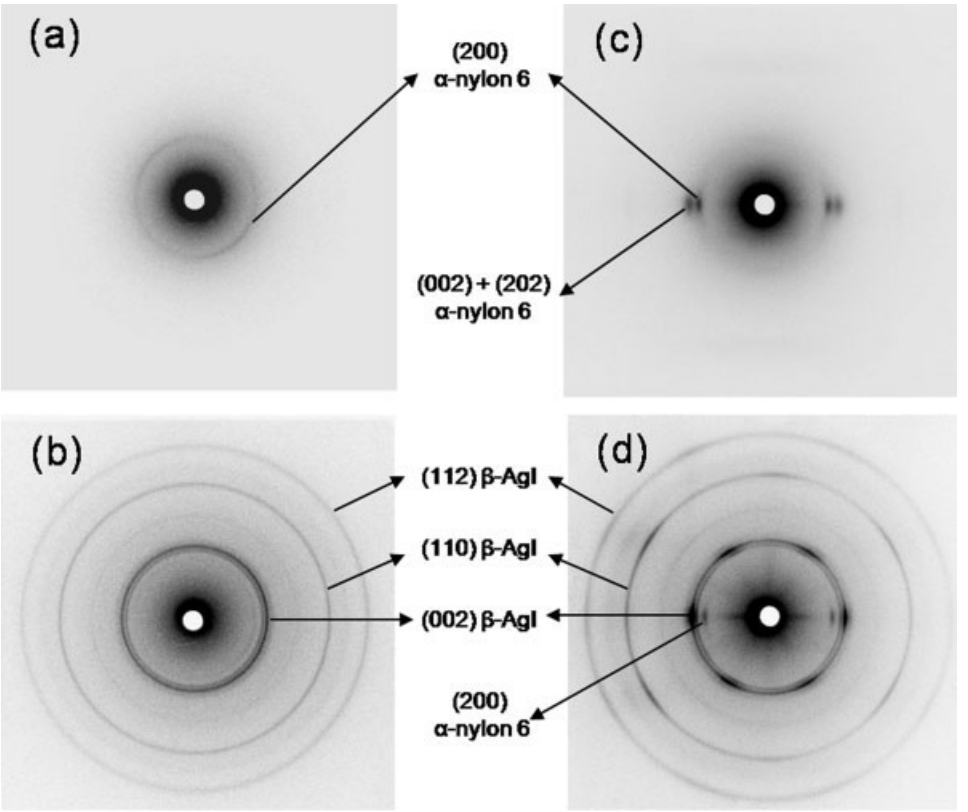

Figure 8 XRD photographs of (a) a random nylon 6 film, (b) a random nylon 6/AgI film, (c) a drawn nylon 6 film, and (d) a uniaxially orientated nylon 6/AgI film. The incident X-ray beam was directed perpendicularly to the film surface.

dependence of the electrical conductivity of a drawn nylon 6/AgI composite film prepared at primary and secondary doping immersion temperatures of 15°C. Open and filled circles show the conductivities parallel ($\sigma_{\parallel}$) and perpendicular ($\sigma_{\perp}$), respectively, to the drawn (chain) axis. The electrical conductivity $\sigma_{\parallel}$ was one order higher than $\sigma_{\perp}$ (There was no measurement direction dependence of conductivity for

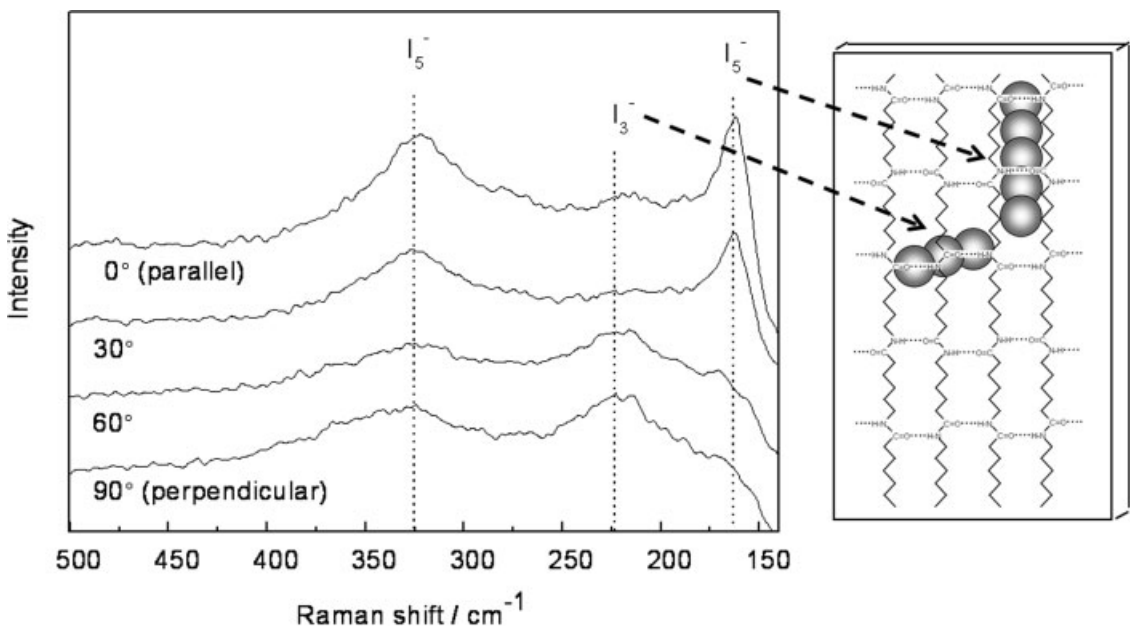

Figure 9 Polarized Raman spectra of drawn nylon 6 films after primary iodine doping. Different angles show the direction between the polarized plane of the laser and the drawing direction of the nylon 6.

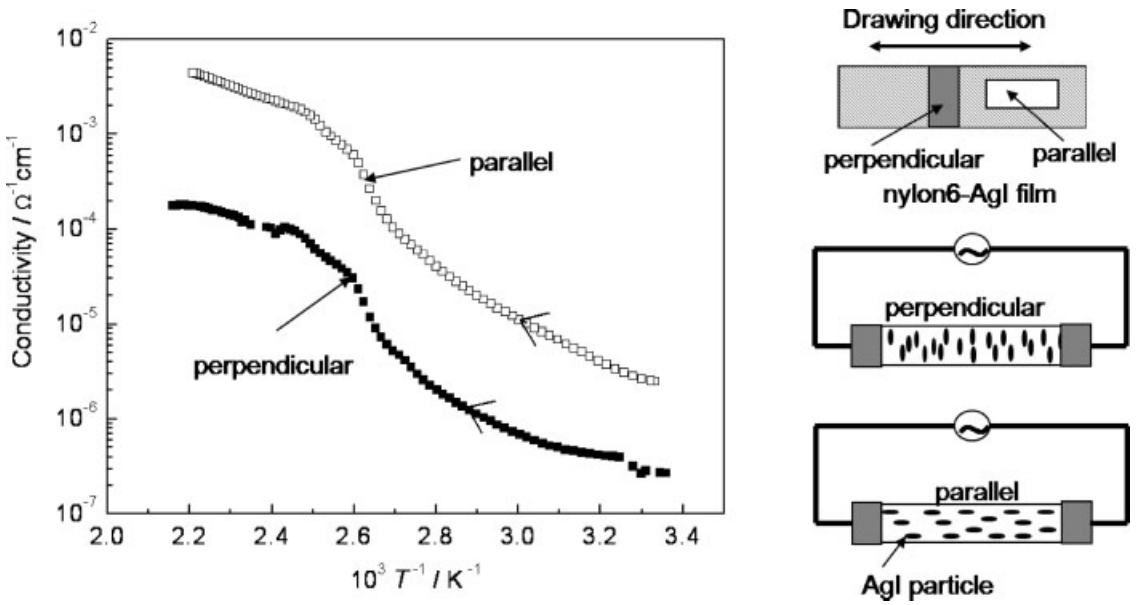

Figure 10 Temperature (T) dependence of the electrical conductivity of the nylon 6/AgI composite: (□) parallel and (■) perpendicular to the drawing direction.

the random nylon 6/AgI composite.). The slopes of the conductivity curves changed above 100°C (ca. 2.7 $\times$ 10^{-3} K^{-1}). This temperature was probably the transition temperature from β-AgI to α-AgI because the conductivity increased due to the transition to highly conductive α-AgI. This was confirmed by differential scanning calorimetry of the drawn composite film, which showed an endothermic peak indicating the crystal transition at about 100°C. In general, the transition temperature from β-AgI to α-AgI is at 147°C, whereas the transition temperature of the drawn nylon 6/AgI composite was shifted to 40°C lower. The lowering of the transition temperature was related to an excess of Ag^+ ions against the stoichiometric composition of AgI, but the detailed reasons for this observation are yet to be clarified and are now under investigation. From the previous results, the nylon 6/AgI composite with anisotropic electrical conductivity was prepared via a complex of oriented polyiodide ions in nylon 6.

Mechanism of AgI formation

The reaction path for polyiodide ions, such as I_3^- and I_5^-, with $AgNO_3$ in nylon 6 is considered next. For I_3^- as an example, two possible pathways can be derived as follows:

$$I_3^- + AgNO_3 \rightarrow AgI + NO_3^- + I_2 \quad \text{(I)}$$

$$I_3^- + 3AgNO_3 + 2e^- \rightarrow 3AgI + 3NO_3^- \quad \text{(II)}$$

For reaction I, the molar ratio of I_3^- (reactant) to AgI (product) in the equation is 3 : 1, whereas for reaction II, the molar ratio is 1 : 1. In the case of I_5^-, the molar ratios are 5 : 1 and 1 : 1 when the reactions proceed in the same manner as reactions I and II, respectively. To clarify the reaction, the relationship between the amounts of iodine in the nylon 6/polyiodide complex and AgI in nylon 6/AgI was investigated by the determination of weight gains after primary and secondary doping. Primary and secondary doping were both carried out at 15°C. As a result, the weight gain by iodine in primary doping was 0.581 to 1 g of original nylon 6 (4.578 mmol/g), whereas the amount of AgI was 1.050 g (4.472 mmol/g)/1 g of original nylon 6. The weight gains by iodine in the primary doping were determined as follows; the weight gain of 0.606 g/g of original nylon 6 was measured after primary doping. This sample contained potassium ions as counter ions. Therefore, thermogravimetric analysis measurement was conducted in an air flow. Only KI remained as ash after heating at 550°C, and the amount of KI introduced into the iodinated nylon 6 was determined as 0.111 g/g of original nylon 6; thus, the amount of K^+ ions was 0.025 g/g of original nylon 6. Consequently, the amount of iodide was 0.581 g against 1 g of original nylon 6.) That is, the molar ratio of I and AgI was approximately 1 : 1. This result supports the approval of reaction II. This was supported by the fact that chromatic I_2 was not observed during the secondary doping reaction. The number of moles of AgI was somewhat lower than that of iodine. This was attributed to the elution of a small amount of AgI into the $AgNO_3$ solution during secondary doping. A supply source of electrons for reaction II to proceed was necessary, but it has not yet been clarified. Both I_3^- and NO_3^-

TABLE I
Antibacterial Properties of Nylon 6 and the Nylon 6/AgI Composite

	Colony-forming units per milliliter			
	Nylon 6 (control)		Nylon 6/AgI	
Bacteria	Initial	After 18 h	Initial	After 18 h
Staphylococcus aureus	8.85×10^3	2.44×10^6	8.85×10^3	<10
Klebsiella pneumoniae	3.87×10^4	4.30×10^7	3.87×10^4	<10
Pseudomonas aeruginosa	4.24×10^4	2.51×10^8	4.24×10^4	<10

ions are strong oxidizing agents and have low possibilities to donate electrons; therefore, we are considering that the electrons were supplied from the matrix polymer.

Antibacterial property

For supplementary data, the antibacterial properties of the composite were examined. Table I represents the resulting data of antibacterial properties against three kinds of bacteria, *Staphylococcus aureus*, *Klebsiella pneumoniae*, and *Pseudomonad aeruginosa*. Neat nylon 6 as a control had no antibacterial properties because the colony forming units for all bacteria were considerably increased after incubation. On the other hand, for nylon 6/AgI, the colony forming units were almost zero, although the amount of included AgI in the composite was considerably limited (only several weight percentage), which indicated that the composite had high bacterial killing properties. AgI is a very insoluble compound in water, and the particles are in the inner part of the nylon 6 matrix; thus, the antibacterial properties could be expected to be persistent for long-time use.

CONCLUSIONS

A nylon 6 film complexed with polyiodide ions was immersed in an aqueous solution of $AgNO_3$, and a composite, including a large amount of β-AgI particles, was successfully obtained. The amount of AgI formed in the matrix was strongly dependent on the temperatures of the immersion solutions. The composite exhibited conductivity on the order of 10^{-5} Ω^{-1} cm^{-1}. In addition, the transparency of the composite prepared at lower immersion temperature was relatively high, although the weight of the AgI content exceeded that of the matrix polymer. In the oriented nylon 6 film, AgI was formed as anisotropic particles and displayed crystallite orientation, which introduced anisotropic conductivity to the composite. This was attributed to the orientation of polyiodide ions, as the precursor of AgI, in the orientated nylon 6 chain. Other interesting properties, strong antibacterial activity and good UV absorption (the data of UV–visible spectroscopy are not shown), were observed, so it can be said that the nylon 6/AgI composite is an attractive material.

The SAXS experiments were performed in the Photon Factory of the High Energy Accelerator Research Organization with the approval number 2006G067. The authors thank Takashi Kanno and Akihisa Furuta for their assistance with the experiments.

References

1. Otterwill, R. H.; Woodbridge, R. F. J Colloid Sci 1961, 16, 581.
2. Berry, C. R. Phys Rev 1967, 161, 848.
3. Saijo, H.; Iwasaki, M.; Tanaka, T.; Matsubara, T. Photogr Sci Eng 1982, 26, 92.
4. Smith, P. V. J Phys Chem Solids 1976, 37, 589.
5. Tubandt, C.; Lorenz, E. Z. Z Phys Chem 1914, 87, 513.
6. Tatsumisago, M.; Shinkuma, Y.; Minami, T. Nature 1991, 354, 217.
7. Owens, B. B.; Argue, G. R. Science 1967, 157, 308.
8. Owens, B. B.; Argue, G. R. J Electrochem Soc 1970, 11, 898.
9. Guo, Y.-G.; Lee, J.-S.; Maier, J. Adv Mater 2005, 17, 2815.
10. Ida, T.; Kimura, K. Solid State Ionics 1998, 107, 313.
11. Validžić, I. L.; Jokanović, V.; Uskoković, D. P.; Nedeljković, J. M. J Eur Ceram Soc 2007, 27, 927.
12. He, H.; Wang, Y.; Chen, H. Solid State Ionics 2004, 175, 651.
13. Uvarov, N. F.; Hairetdinov, E. F.; Bokhonov, B. B.; Bratel, N. B. Solid State Ionics 1996, 86, 573.
14. Chen, S. H.; Ida, T.; Klimura, K. J Phys Chem B 1998, 102, 6169.
15. Rotstein, H.; Tannenbaun, R. In Synthesis, Functionalization and Surface Treatment of Nanoparticles; Baraton, M. I., Ed.; American Scientific Publishers: California, 2003; p 103.
16. Caseri, W. Macromol Rapid Commun 2000, 21, 705.
17. Bradley, J. S. In Clusters and Colloids; Schmid, G., Ed.; VCH: Weinheim, 1994; p 523.
18. Mayer, A. B. R. Polym Adv Technol 2001, 12, 96.
19. Gubin, S. P. Colloids Surf A 2002, 202, 155.
20. Gotoh, Y.; Kanno, T.; Fujimori, Y.; Ohkoshi, Y.; Nagura, M.; Akamatsu, K.; Deki, S. Polym J 2003, 35, 960.
21. Fujimori, Y.; Gotoh, Y.; Kohda, Y.; Nagura, M.; Ohkoshi, Y. Sen'i Gakkaishi (in Japanese) 2004, 60, 237.
22. Fujimori, Y.; Gotoh, Y.; Tamaki, N.; Ohkoshi, Y.; Nagura, M. J Mater Chem 2005, 15, 4816.
23. Wang, Y.; Ye, C.; Wang, G.; Zhang, L. Appl Phys Lett 2003, 82, 4253.
24. Gotoh, Y.; Kanno, T.; Ohkoshi, Y.; Nagura, M.; Akamatsu, K.; Mizuhata, M.; Deki, S. Proc Int Symp Small Part Inorg Clusters 2002, 11, B-XII-8.
25. Joint Committee on Powder Diffraction Standards, File No. 9–374.
26. Abu-Isa, I. A. J Appl Polym Sci 1971, 15, 2865.
27. Yoshida, K.; Endo, M. Kogyo Kagaku Zasshi (in Japanese) 1956, 59, 1074.

28. Shahi, K.; Wagner, J. B., Jr. J Electrochem Soc 1981, 128, 6.
29. Beran, M. J. P. Statistical Continuum Theories; Wiley-Interscience: New York, 1968; p 181.
30. Shapiro, I.; Kolthoff, I. M. J Chem Phys 1947, 15, 41.
31. Jow, T.; Wagner, J. B., Jr. J Electrochem Soc 1979, 126, 1963.
32. CRC Handbook of Chemistry and Physics, 76th ed.; Lide, D. R., Ed.; CRC: Boca Raton, FL, 1995; p 4.
33. Polymer Handbook, 3rd ed.; Brandrup, J.; Immergut, E. H., Eds.; Wiley: Toronto, 1989; p V–114.
34. Takada, S. Jpn J Appl Phys 1973, 12, 190.
35. Lee, J.-S.; Adams, S.; Maier, J. Solid State Ionics 2000, 136, 1261.
36. Lee, J.-S.; Adams, S.; Maier, J. J Electrochem Soc 2000, 147, 2407.
37. Davis, B. L.; Petersen, R. L. Cryst Lattice Defects 1970, 1, 275.
38. Davis, B. L.; Petersen, R. L. Cryst Lattice Defects 1974, 5, 235.
39. Kawaguchi, A.; Tsurutani, N.; Miyaji, H. Spring-8 User Exp Rep 2000, 5, 354.
40. Murthy, N. S. Macromolecules 1987, 20, 309.
41. Kawaguchi, A. Polymer 1992, 33, 3981.
42. Murthy, N. S.; Szollosi, A. B.; Sibilia, J. P.; Krimm, S. J Polym Sci Polym Phys Ed 1985, 23, 2369.
43. Burzynski, R.; Prasad, P. N.; Murthy, N. S. J Polym Sci Part B: Polym Phys 1986, 24, 133.
44. Lee, Y. H.; Porter, R. S. J Macromol Sci Phys B 1995, 34, 295.
45. Fujimori, Y. Unpublished data.